Role of coupling and zeolite Acidity in the Methanol-mediated CO_2 Conversion to Olefins over ZnZrO*x*-AEI Zeolite Tandem Catalysis

Ahmed Sajid[1], Julien Devos[1], Sven Robijns[1], Thibaut Donckels[1], Ibrahim Khalil[1], Michiel Dusselier[1*]*

[1]Center for Sustainable Catalysis and Engineering (CSCE), KU Leuven, Celestijnenlaan 200F, B-3001 Leuven, Belgium

Supplementary info

Contents

1. Materials and Methods 2
   1.1. Steaming 2
2. Characterization 3
   2.1. X-ray diffraction 3
   2.2. N_2-physiosorption 3
   2.3. Calculation for methanol adsorption and retention capacity based on area under peaks of FT-IR spectra 4
   2.4. NH_3-TPD: 5
   2.5. Solid state ^{27}Al NMR 5
   2.6. Raman Spectroscopy 6
   2.7. Thermogravimetric analysis (TGA) 6
3. Catalytic activity results 7
4. Noise reduction 12
5. Alumina positions in zeolite framework 12
6. References 13

1. Materials and Methods

1.1. Steaming

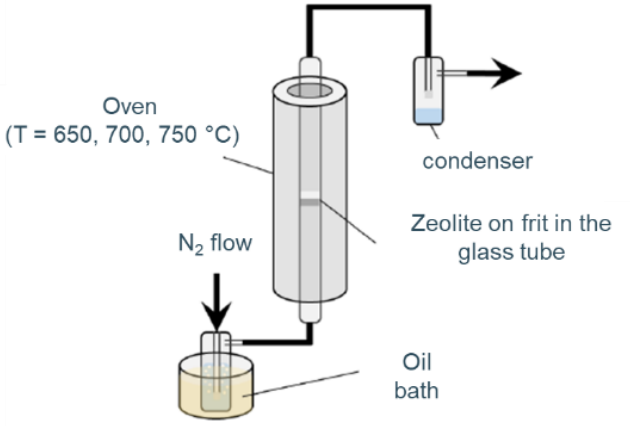

Figure S1: Schematic showing the set-up for post synthetic steaming treatment of the SSZ-39 and SAPO-18 zeolite(type). The nitrogen first passes through the bubbler containing the MQ water (18.2 MΩ, filtered through Synergy UV purification system) at room temperature and then to the heated bubbler placed in oil bath. The oil bath is heated over a magnetic hot plate and the temperature of the oil bath is controlled at 80 °C by the thermocouple. Nitrogen takes up the saturated steam bubbles from this heated bubbler before entering the steaming oven. The temperature of the steaming oven is also controlled by the thermocouple placed close to the frit where zeolite(type) sample was placed. Before starting the experiment, the temperature of the steaming oven was controlled at 105 °C to prevent the condensation of the saturated vapors. At the end, the exhaust line is connected with the condenser to prevent the condensation inside the steaming set-up and to avoid the pressure build up. Finally the steaming was carried out as per the procedure mentioned in the main article.

2. Characterization

2.1. X-ray diffraction

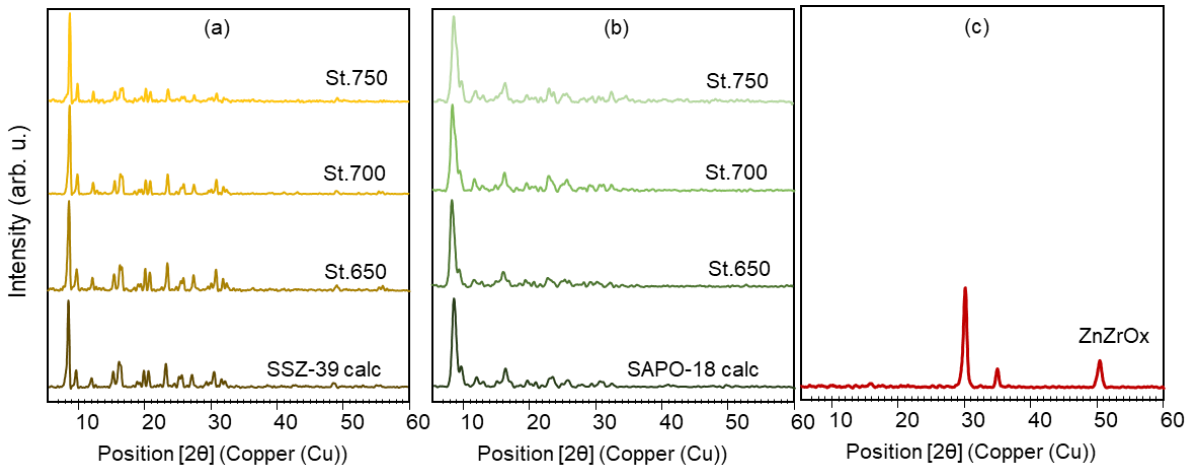

Figure S2: Powder (XRD) spectra for calcined (un-steamed) and steamed (a) SSZ-39 (b) SAPO-18 catalysts and (c) metal oxide ZnZrOx

2.2. N_2-physiosorption

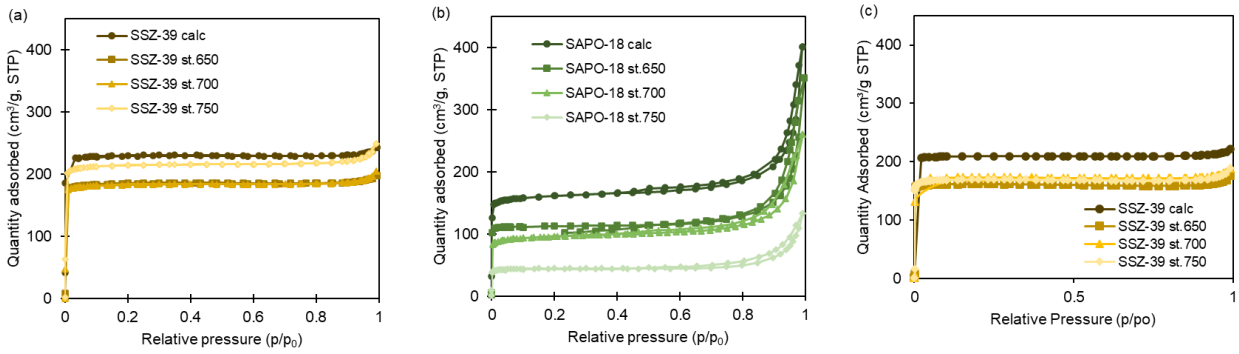

Figure S3: Structural changes observed on steaming (a) SSZ-39 and (b) SAPO-18 as measured by N_2 physisorption, (c) to check re-producibility in trends observed in panel (a), the N_2 physisorption over another synthesis batch was done and results are shown in panel (c), with different values of micropore volume, the trend is similar except that the decrease in micropore volume for st.750 in this batch was higher than earlier. However, the difference between micropore volume of calcined and st.750 reported in our work is closely in line with earlier work by Dusselier *et al [1]*.

Table S1: BET surface area[1] and composition[2] of ZnZrOx catalyst used in this work

Structural parameter	Estimated value
BET surface area	49 m^2 g_{cat}^{-1}
Zn loading	12 wt. %

2.3. Calculation for methanol adsorption and retention capacity based on area under peaks of FT-IR spectra

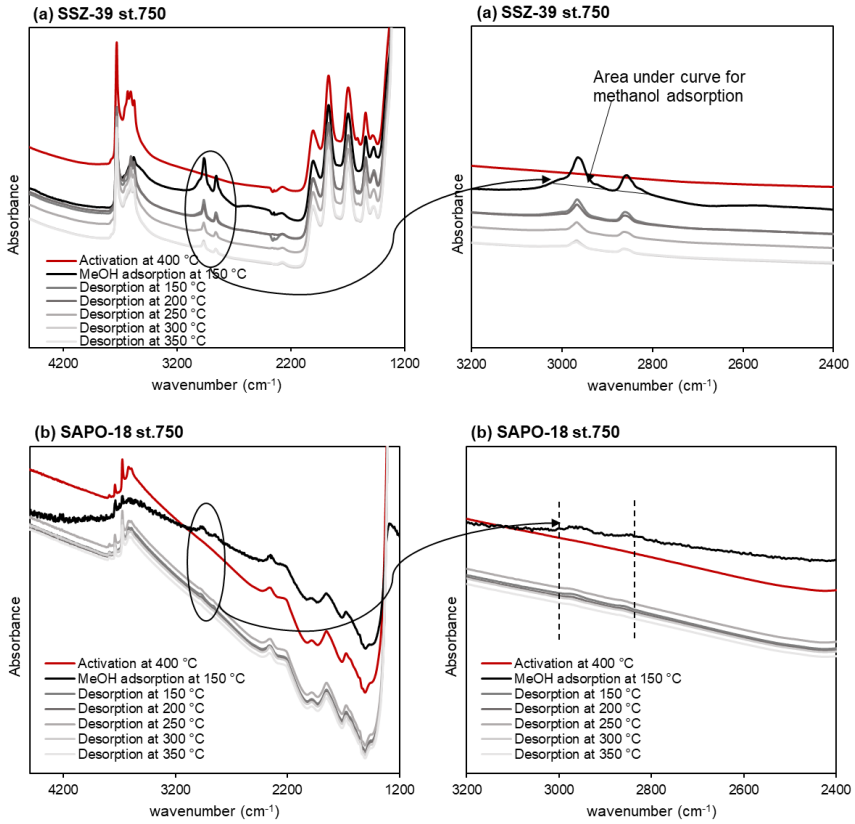

Figure S4: Top: FT-IR spectra of SSZ-39 st.750 showing the peaks for methanol and illustration to shows how the area under curve for methanol adsorption and then for subsequent desorption at different temperatures was calculated, bottom: similar procedure for SAPO-18 st.750. Note: The calculation above are shown for two samples, same procedure was repeated to calculate the methanol adsorption and retention capacity for all samples mentioned in this article.

[1] Calculated by N_2-physiosorption

[2] Estimated from inductively coupled plasma-optical emission spectroscopy (ICP-OES)

2.4. NH_3-TPD:

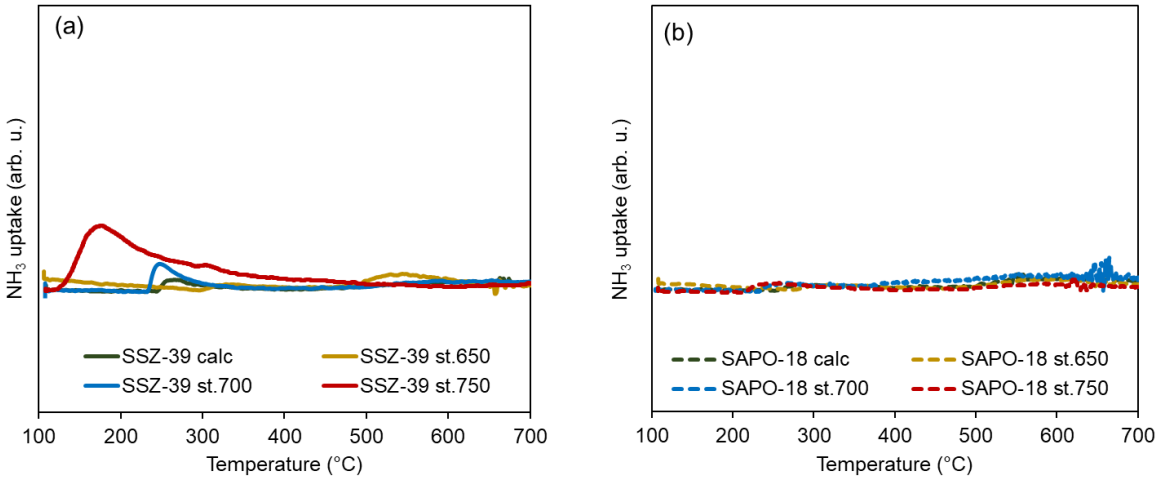

Figure S5: TPD profiles of un-steamed and steamed (a) SSZ-39 (b) SAPO-18. The samples were treated in 99.999% He as mentioned in Section 2.2. After treatment step, the samples were allowed to undergo temperature desorption from 100-700 °C in the presence of He. No probe was used to saturate the samples while performing blank TPD measurements. The Savitzky-golay function in python with window size and order of 51 and 6 respectively was used to smooth the curves.

2.5. Solid state ^{27}Al NMR

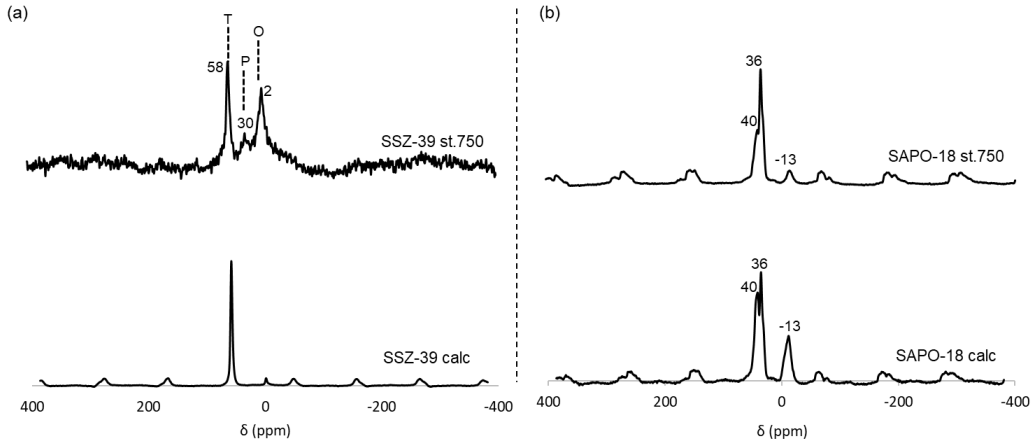

Figure S6: Solid state ^{27}Al NMR for unsteamed and st.750 samples of (a) SSZ-39 and (b) SAPO-18. T = tetrahedral, p = pentahedral and o = octahedral alumina. Panel 9(a) shows the appearance of octahedral and pentahedral coordinated aluminum species on steaming, while reducing the tetrahedral species [1]. Panel (b) shows the peak at -13 ppm, which possibly represents octahedral coordinated extra framework aluminum species, while the peaks appearing at the signal shift of 36 and 40 ppm represents the tetrahedral coordinated framework alumina species $Al(OP)_4$ [2–4].

2.6. Raman Spectroscopy

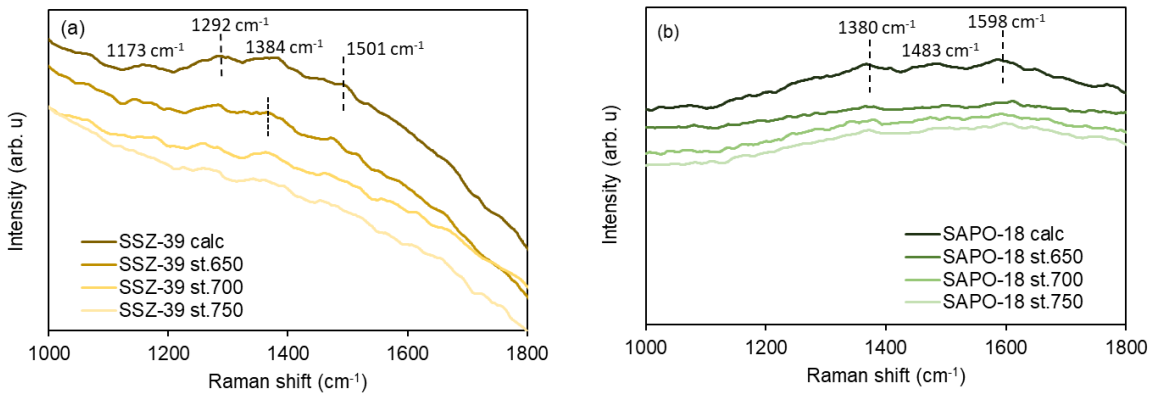

Figure S7: Raman spectra of spent un-steamed and steamed catalysts (a) SSZ-39 (b) SAPO-18. The Savitzky-golay function in python with window size and order of 51 and 6 respectively was used to smooth the curve.

2.7. Thermogravimetric analysis (TGA)

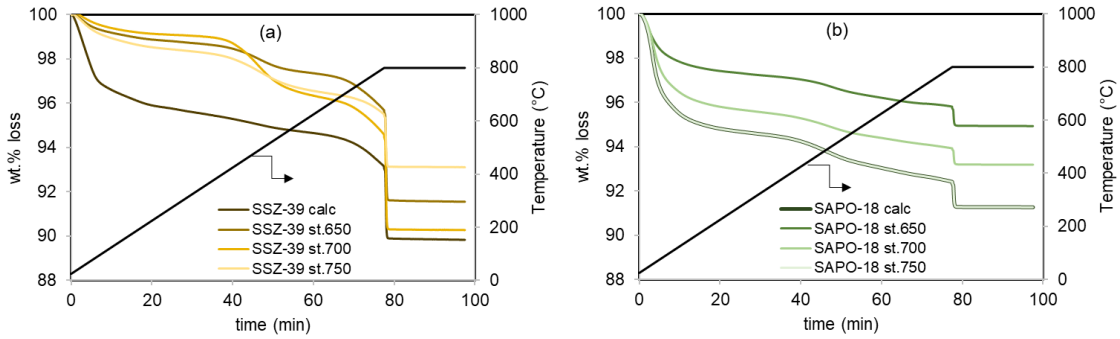

Figure S8: TGA curves for spent un-steamed and steamed zeolite(type) samples: (a) SSZ-39 (b) SAPO-18

Table S2: Percentage weight loss from spent un-steamed and steamed catalyst + ZnZrOx

Zeolite(type) + ZnZrOx	Water loss (wt. %)	Soft cokes	Hard cokes
SSZ-39 calc	3.4%	3.4%	3.1%
SSZ-39 st.650	0.82%	3.5%	3.9%
SSZ-39 st.700	0.62%	4.9%	4.1%
SSZ-39 st.750	1.1%	3.4%	2.2%
SAPO-18 calc	4.5%	3.2%	1.1%
SAPO-18 st.650	2.2%	2.1%	0.80%
SAPO-18 st.700	3.6%	2.6%	0.7%
SAPO-18 st.750	3.3%	2.3%	0.62%

3. Catalytic activity results

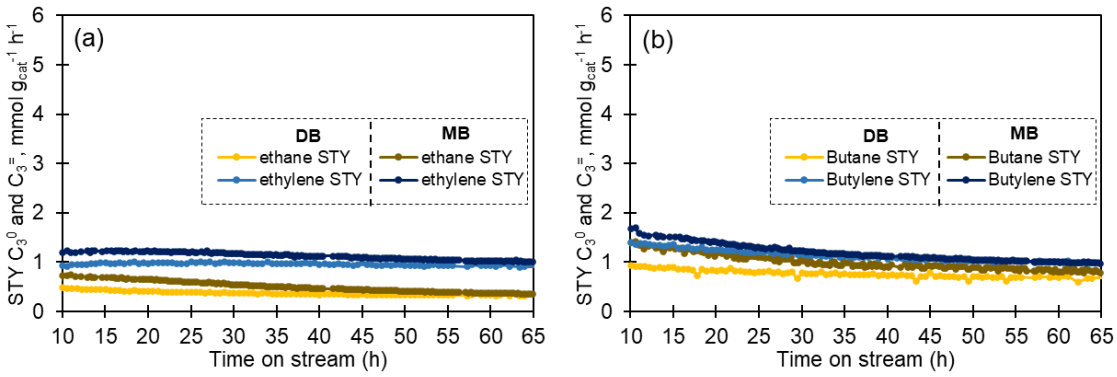

Figure S9: Comparison between productivity of C2 and C4 hydrocarbons in dual bed and mixed bed system. Reaction conditions: T = 380 °C, P = 4.0 MPa, GHSV = 18000 ml g_{cat}^{-1} h^{-1}, H_2/CO_2 = 3.0, carbon balance (CB) = 98-100%.

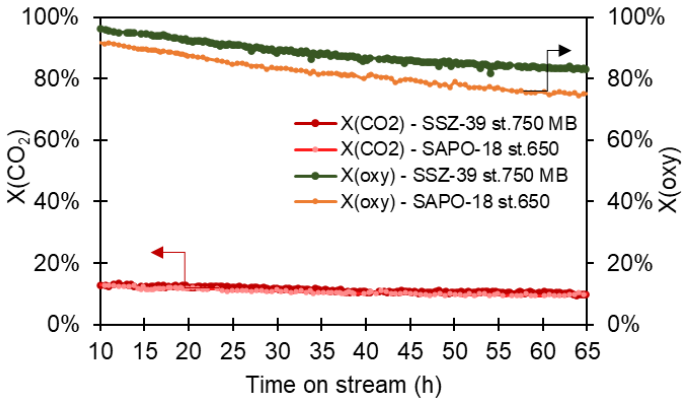

Figure S10: Comparison in terms of stability between ZnZrOx + (SSZ-39 st.750 and SAPO-18 st.650) performance in terms of oxygenate conversion in mixed bed configuration. Reaction conditions: T = 380 °C, P = 4.0 MPa, GHSV = 18000 ml g_{cat}^{-1} h^{-1}, H_2/CO_2 = 3.0, carbon balance (CB) = 98-100%.

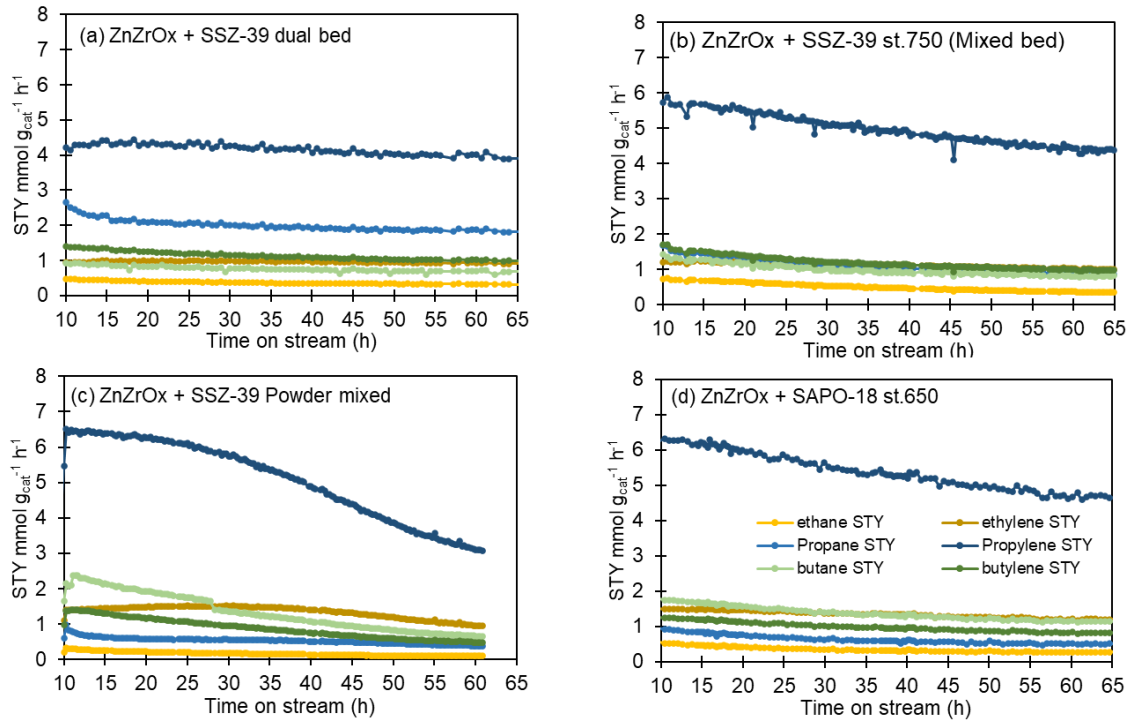

Figure S11: Space time yields of C2, C3 and C4 hydrocarbons over tandem ZnZrOx + (a) SSZ-39 st.750 dual bed (b) SSZ-39 st.750 mixed bed (c) SSZ-39 st.750 powder mixed and (d) SAPO-18 st.650 catalysts. Reaction conditions: T = 380 °C, P = 4.0 MPa, GHSV = 18000 ml g_{cat}^{-1} h^{-1}, H_2/CO_2 = 3.0, carbon balance (CB) = 98-100%.

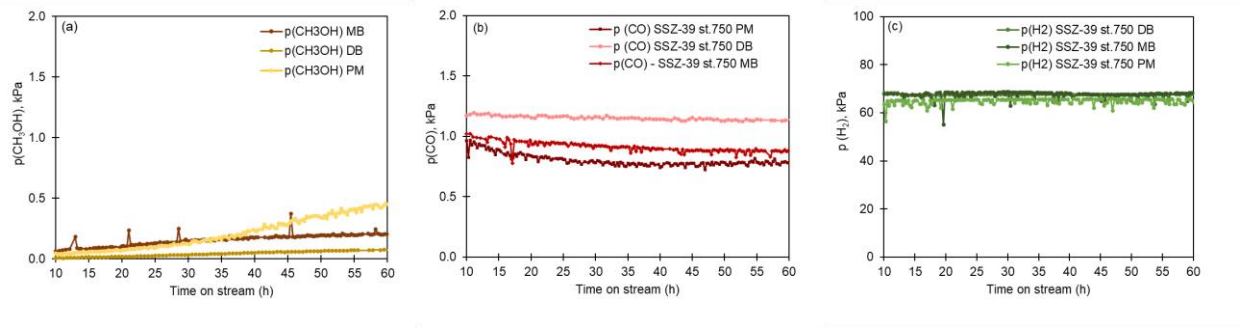

Figure S12: Comparison of partial pressure of (a) methanol (b) carbon monoxide and (c) hydrogen in the product stream between tandem ZnZrOx + SSZ-39 st.750 catalysts in dual bed (DB), Mixed bed (MB) and powder mixed (PM) configuration. Reaction conditions: T = 380 °C, P = 4.0 MPa, GHSV = 18000 ml g_{cat}^{-1} h^{-1}, H_2/CO_2 = 3.0, carbon balance (CB) = 98-100%.

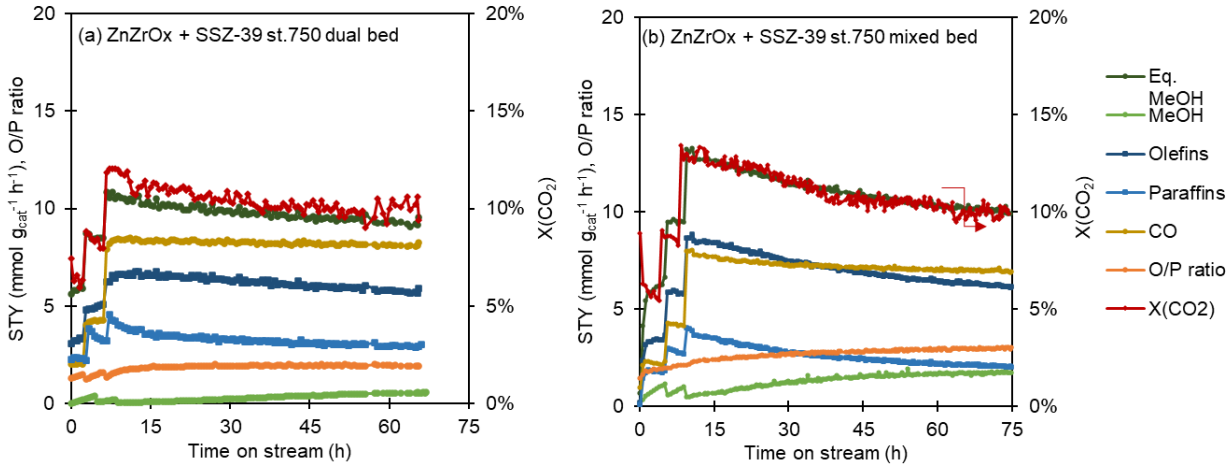

Figure S13: Catalytic activity over SSZ-39 st.750 + ZnZrOx in (a) dual bed and (b) mixed bed configuration at different reaction temperatures. Reaction conditions: *T* = 380 °C, *P* = 4.0 MPa, GHSV = 18000 ml g_{cat}^{-1} h^{-1}, H_2/CO_2 = 3.0, carbon balance (CB) = 98-100%.

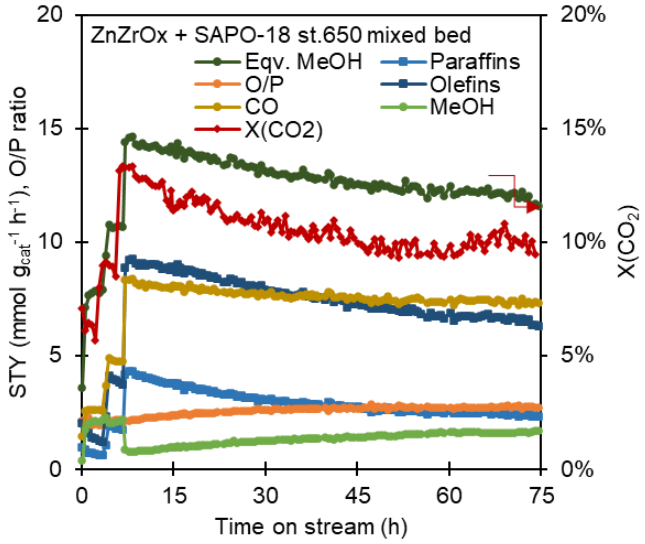

Figure S14: Catalytic activity over SAPO-18 st.650 + ZnZrOx in b mixed bed configuration at different reaction temperatures. Reaction conditions: *T* = 380 °C, *P* = 4.0 MPa, GHSV = 18000 ml g_{cat}^{-1} h^{-1}, H_2/CO_2 = 3.0, carbon balance (CB) = 98-100%.

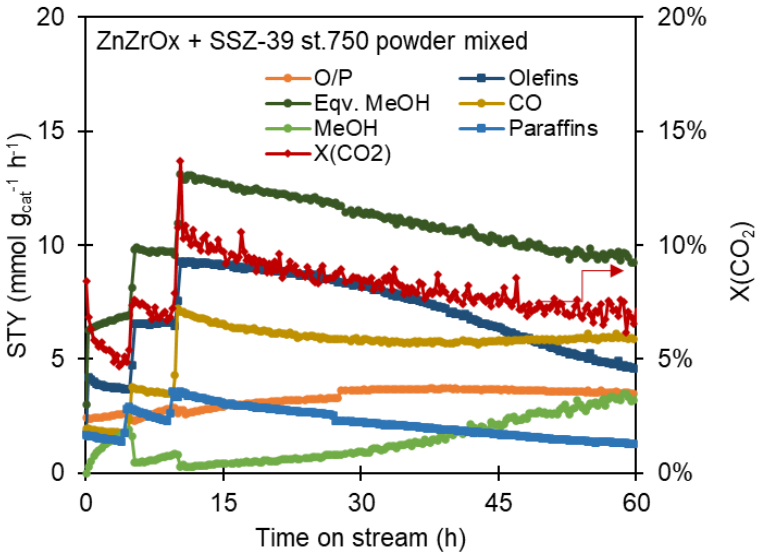

Figure S15: Summary of catalytic activity over SSZ-39 st.750 + ZnZrOx in powder mixed configuration at different reaction temperatures. Reaction conditions: T = 380 °C, *P* = 4.0 MPa, GHSV = 18000 ml g_{cat}^{-1} h^{-1}, H_2/CO_2 = 3.0, carbon balance (CB) = 98-100%.

.

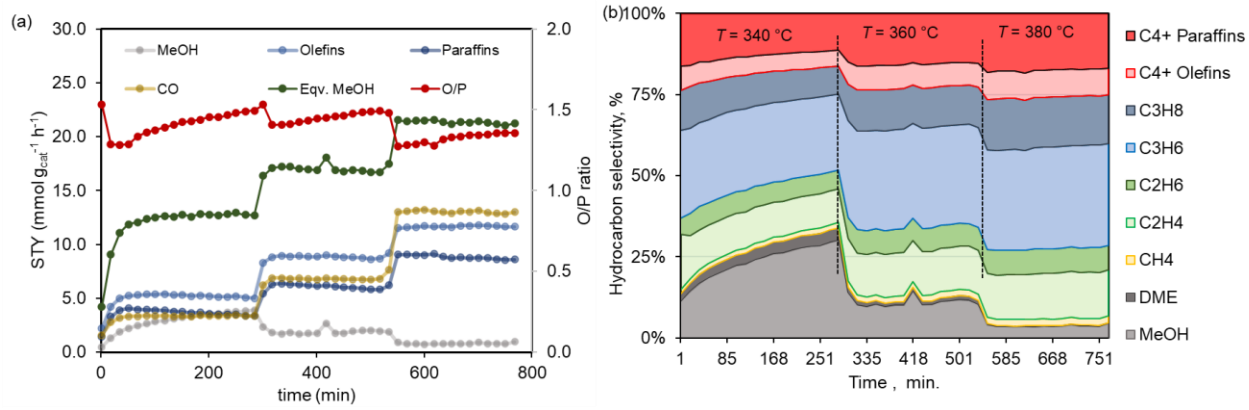

Figure S16: Summary of catalytic activity over SSZ-13 (Si/Al = 68) + ZnZrOx in mixed bed configuration at different reaction temperatures. (a) STY of products and olefin/paraffin ratio (b) product selectivity among hydrocarbons and oxygenates at different reaction steps. Reaction conditions: T = 380 °C, *P* = 4.0 MPa, GHSV = 18000 ml g_{cat}^{-1} h^{-1}, H_2/CO_2 = 3.0, carbon balance (CB) = 98-100%. Olefin/paraffin ratio of 1.3 at *T* = 380 °C was observed on a CHA topology zeolite as compared to the SSZ-39 st.750 (O/P ratio 2.1 at *T* = 380 °C), showing the superior performance of SSZ-39 st.750. Further, propylene selectivity in SSZ-13 was observed to be lower (31%, Figure S16(b)) than what was observed in SSZ-39 st.750.

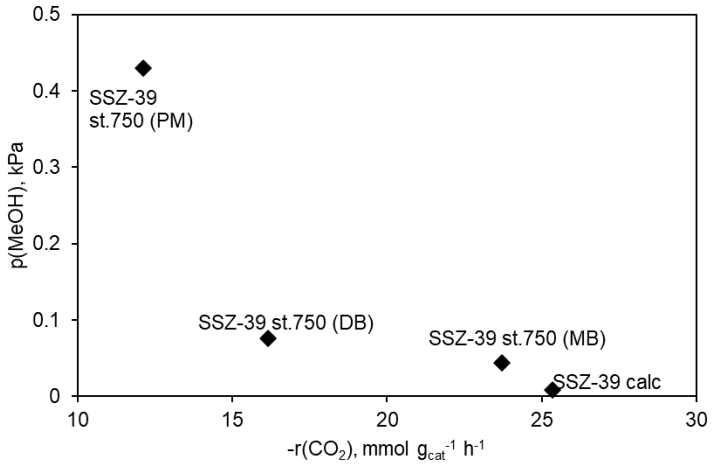

Figure S17: Variation of partial pressure of methanol in product stream vs. rate of CO_2 conversion over SSZ-39 (calc and st.750) combined with ZnZrOx in different configurations. The -rCO_2 and p(MeOH) values for powder mixed (PM) and dual bed (DB) were averaged over the last 10 hours of reaction on time on stream. Reaction conditions: T = 380 °C, *P* = 4.0 MPa, GHSV = 18000 ml g_{cat}^{-1} h^{-1}, H_2/CO_2 = 3.0, carbon balance (CB) = 98-100%.

Table S3: Results showing kinetic coupling between Carbon dioxide to methanol (CTM) and methanol to olefins (MTO) reaction during tandem carbon dioxide conversion to olefins. The CTM reaction is a separate reaction on only ZnZrOx run in exactly the same conditions except GHSV = 27000 ml g_{cat}^{-1} h^{-1} which is equal to that of ZnZrOx during tandem MOx + zeolite system. Tio keep the same GHSV, 300 mg of ZnZrOx was used in CTM and the flows were adjusted accordingly to achieve same GHSV. CTO reaction conditions: T = 340, 360, 380 °C, P = 4.0 MPa, GHSV = 18000 ml g_{cat}^{-1} h^{-1}, H_2/CO_2 = 3.0, carbon balance (CB) = 98-100%.

Reaction Temperature (°C)	STY (mmol g_{cat}^{-1} h^{-1}), X(CO_2)	CTM (ZnZrOx)	Tandem CTO (ZnZrOx + SSZ-39 st.750)		Tandem CTO (ZnZrOx + SAPO-18 st.650)	
		Experimental	Experimental	Weight corrected	Experimental	Weight corrected
340	Eq. MeOH	11	6.6	9.9	8.8	13
	CO	3.1	2.4	3.6	2.0	3.0
	X (CO_2)	5.4%	6.5%	-	6.8%	-
360	Eq. MeOH	13	10	15	12	18
	CO	6.7	4.5	6.8	3.9	5.9
	X (CO_2)	7.4%	9.1%	-	9.3%	-
380	Eq. MeOH	10	14	21	15	23
	CO	14	8.4	13	7.3	11
	X (CO_2)	9.2%	14%	-	13%	-

Table S4: Example of the calculation for the WHSV MTO mentioned in the Table 2 of main text

Catalyst	STY (mmol C g_{cat} h^{-1})*	WTY $kg_{Eq.MeOH}$ kg_{cat}^{-1} h^{-1}	WHSV × 3 (Weight corrected for zeolite)
ZnZrOx + SSZ-39 st.750 dual bed	10.8 (Ref: Fig S10 A)	0.34	1.04
ZnZrOx + SSZ-39 st.750 mixed bed	13.2 (Ref: Fig S10 B)	0.42	1.26 ≈ 1.3
ZnZrOx + SSZ-39 st.750 powder mixed	13.1 (Ref: Fig S12)	0.41	1.23 ≈ 1.2
ZnZrOx + SAPO-18 st.750 mixed bed	14.1 (Ref: Fig S11)	0.45	1.35 ≈ 1.3

*Eq. MeOH from figures

4. Noise reduction

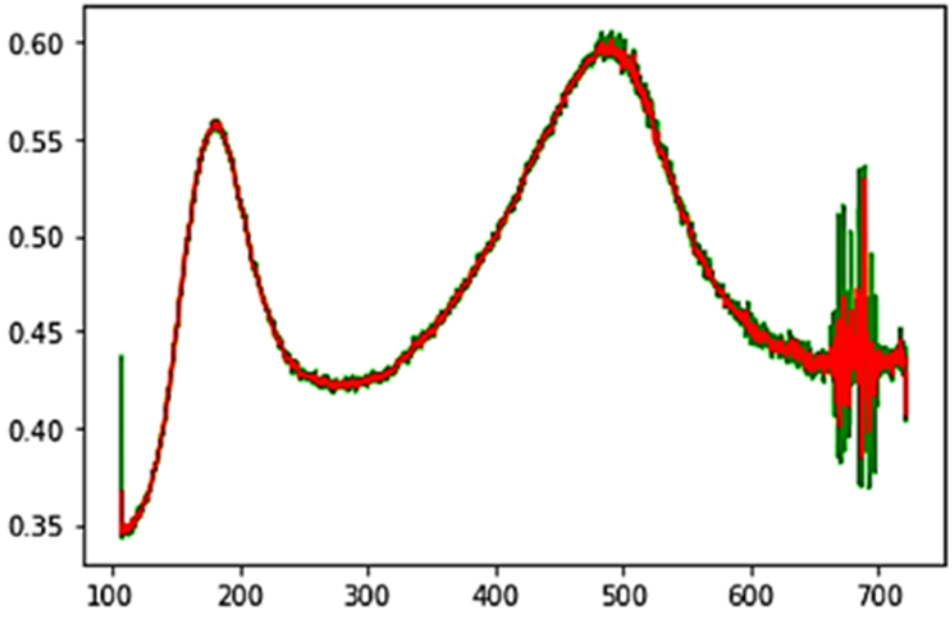

Figure S18: An example of noise reduction by The Savitzky-golay function in python with window size and order of 51 and 6 to smooth the curves.

5. Alumina positions in zeolite framework

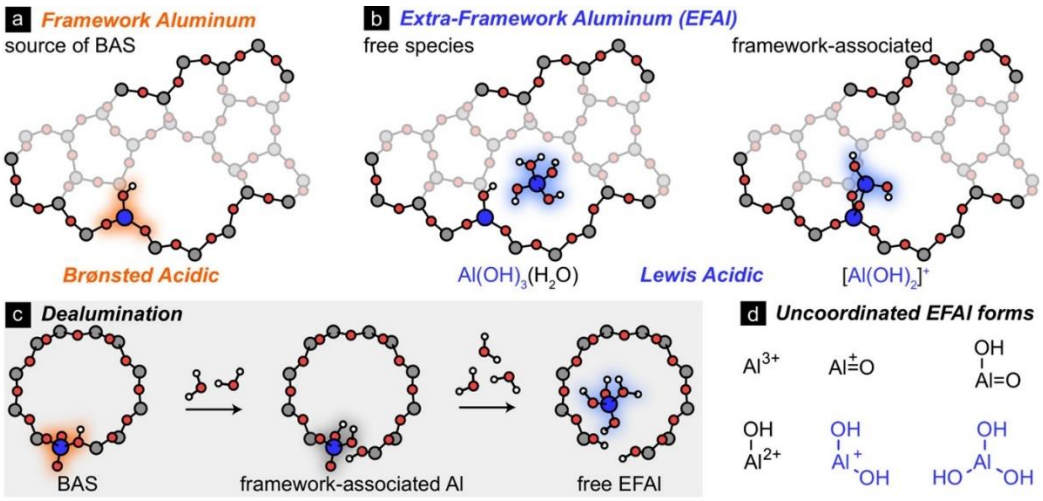

Figure S19: Representation of location and coordination environment of alumina species in zeolite. Scheme from the work of Mancuso *et al*. [5]. Reused with permission from Elsevier, copyright 2024.

6. References

[1] M. Dusselier, M.A. Deimund, J.E. Schmidt, M.E. Davis, Methanol-to-Olefins Catalysis with Hydrothermally Treated Zeolite SSZ-39, ACS Catal 5 (2015) 6078–6085. https://doi.org/10.1021/acscatal.5b01577.

[2] A. Buchholz, W. Wang, A. Arnold, M. Xu, M. Hunger, Successive steps of hydration and dehydration of silicoaluminophosphates H-SAPO-34 and H-SAPO-37 investigated by in situ CF MAS NMR spectroscopy, n.d. www.elsevier.com/locate/micromeso.

[3] A. Buchholz, W. Wang, M. Xu, A. Arnold, M. Hunger, Thermal stability and dehydroxylation of Brønsted acid sites in silicoaluminophosphates H-SAPO-11, H-SAPO-18, H-SAPO-31, and H-SAPO-34 investigated by multi-nuclear solid-state NMR spectroscopy, n.d. www.elsevier.com/locate/micromeso.

[4] Z. Li, J. Martínez-Triguero, J. Yu, A. Corma, Conversion of methanol to olefins: Stabilization of nanosized SAPO-34 by hydrothermal treatment, J Catal 329 (2015) 379–388. https://doi.org/10.1016/j.jcat.2015.05.025.

[5] J.L. Mancuso, V. Van Speybroeck, The nature of extraframework aluminum species and Brønsted acid site interactions under catalytic operating conditions, J Catal 429 (2024). https://doi.org/10.1016/j.jcat.2023.115211.